Precambrian Research 182 (2010) 43–56

Contents lists available at ScienceDirect

Precambrian Research

journal homepage: www.elsevier.com/locate/precamres

Geochemistry of TTG and TTG-like gneisses from Lushan-Taihua complex in the southern North China Craton: Implications for late Archean crustal accretion

Xiao-Long Huang[a,*], Yaoling Niu[b], Yi-Gang Xu[a], Qi-Jun Yang[a], Jun-Wei Zhong[a]

[a] Key Laboratory of Isotope Geochronology and Geochemistry, Guangzhou Institute of Geochemistry, Chinese Academy of Sciences, Guangzhou 510640, China
[b] Department of Earth Sciences, Durham University, Durham DH1 3LE, UK

ARTICLE INFO

Article history:
Received 24 July 2009
Received in revised form 21 June 2010
Accepted 23 June 2010

Keywords:
Grey gneisses
TTG and TTG-like gneisses
Amphibolite
Crustal accretion
Flat subduction
Late Archean
North China Craton

ABSTRACT

The Late Archean Taihua complex, mainly composed of amphibolite and TTG and TTG-like gneisses, is volumetrically most important metamorphic rock suites scattered along the southern margin of the North China Craton (NCC). Zircon SHRIMP U–Pb dating shows two episodes (2765 ± 13 and 2723 ± 9 Ma) of Archean magmatism in the Lushan area with distinct geochemical features. The early (2765 ± 13 Ma) suite (TTG-like gneisses) has low-SiO_2 (52.5–66.1 wt%), high-$Mg^{\#}$ (0.47–0.68), low HREE (Yb_N = 3.0–5.4) and Y (8.07–13.9 ppm) with low to moderate $(La/Yb)_N$ (6.7–37.1) and Sr/Y (25.9–119.3). The younger (2723 ± 9 Ma) suite (TTG gneisses) has high-SiO_2 (63.5–74.3 wt%), low-$Mg^{\#}$ (0.13–0.52), very low REE (Yb_N < 1.8) and Y (<4 ppm) with a wide range of $(La/Yb)_N$ (5.2–86.6), Sr/Y (71.4–949) and showing $Eu/Eu^* > 1$ (1.20–2.43). Both suites show pronounced negative Nb–Ta and Ti anomalies on the primitive mantle-normalized spidergram. The TTG-like gneiss suite has similar bulk-rock Nd and zircon Hf model ages (~3.0 Ga) with $\varepsilon_{Nd}(t) > 0$ (0.26–1.46), and is interpreted as resulting from melt of mantle interactions with the melts derived from partial melting of subducted ocean crust with a residual assemblage of garnet + clinopyroxene + rutile ± amphibole, which favors subducted slab model for the late Archean TTG. The TTG gneiss suite has abundant relic zircons (2.95–2.80 Ga) with $\varepsilon_{Nd}(t) < 0$ (−1.31 to −0.23), which is best interpreted as derived from partial melting of thickened lower continental crust with a garnet-amphibolite residue (garnet + amphibole ± rutile). Significant high-pressure fractional crystallization (garnet ± amphibole) and accumulation (plagioclase) are also required in the petrogenesis. The Lushan amphibolite with nearly flat primitive mantle-normalized trace-element pattern is interpreted to represent early ocean crust metamorphism. These observations suggest a possible model of late Archean crustal accretion from ocean crust to continental terrain in the southern North China Craton.

1. Introduction

The tonalite–trondhjemite–granodiorite (TTG) suite (Jahn et al., 1981) volumetrically dominates in the preserved Archean crust (Martin et al., 2005; Smithies et al., 2009), and records the origin and evolution of continental crust in Earth's early history (Martin, 1994; Foley et al., 2002; Martin et al., 2005; Condie, 2005; Smithies et al., 2009). It is commonly accepted that TTGs represent partial melts of hydrous mafic rocks at pressures high enough to stabilize garnet ± amphibole, thus producing tonalitic melts with a characteristic signature of high La/Yb and Sr/Y ratios (e.g., Barker and Arth, 1976; Martin, 1999; Drummond and Defant, 1990; Rapp et al., 1991; Smithies and Champion, 2000; Smithies, 2000; Martin et al., 2005; Condie, 2005). However, debate remains on both tectonic setting and actual processes of melting for TTGs, especially for those in the late Archean (Martin, 1999; Smithies and Champion, 2000; Smithies, 2000; Foley et al., 2002; Martin et al., 2005; Condie, 2005). Geochemical features of TTGs changed over the period from the Early to Late Archean (Martin et al., 2005; Condie, 2005), thus a critical issue related to TTGs is whether and how their genetic mechanism may have changed with time (Condie, 2005; Smithies et al., 2009). Furthermore, late Archean TTGs were also thought to form principally above subduction zones because of the chemical similarities between Late Archean TTGs and present-day adakites (e.g., Drummond and Defant, 1990; Drummond et al., 1996; Martin, 1999; Rapp et al., 2003; Martin et al., 2005), but this interpretation remains a hypothesis to be tested (Bédard, 2006; van Hunen et al., 2008).

The North China Craton (NCC) is the largest and oldest known cratonic block in China (~3.8 Ga; Wu et al., 2008, and references therein), with widespread Archean to Paleoproterozoic basement (Fig. 1a). The Taihua complex, mainly composed of amphibolites and grey gneisses, is volumetrically the most important metamorphic rock suite in the southern NCC (Zhang et al., 1985; Wu et al., 1998; Tu, 1998; Wan et al., 2006). Similar to the Archean grey orthogneiss complexes in West Greenland (Steenfelt et al., 2005),

* Corresponding author. Tel.: +86 20 85290010; fax: +86 20 85291510.
E-mail address: xlhuang@gig.ac.cn (X.-L. Huang).

0301-9268/$ – see front matter © 2010 Elsevier B.V. All rights reserved.
doi:10.1016/j.precamres.2010.06.020

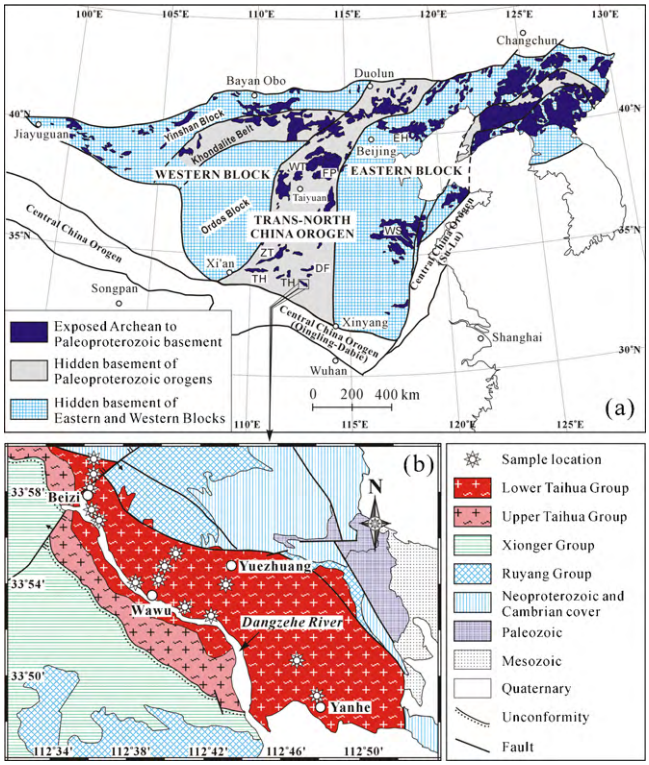

Fig. 1. (a) Tectonic framework of North China Craton (NCC) emphasizing Eastern Block, Western Block, Trans-North China Orogen and exposed Archean to Paleoproterozoic basement (after Zhao et al., 2005); the Taihua Group (TH) and the Dengfeng Group (DF) metamorphic complexes are distributed at the southern margin of the NCC. Abbreviations of other metamorphic complexes: Zhongtiaoshan (ZT), Wutaishan (WT), Fupin (FP), Western Shandong (WS), Eastern Hebei (EH); (b) geological map of the Lushan region, illustrating the distribution of the Taihua group and sample locations. Modified after the Lushan geological map of 1/200,000 scale (BGMR, 1965).

the grey gneisses from the Taihua complex are also dominated by TTG and TTG-like gneisses (Wu et al., 1998; Tu, 1998; Wan et al., 2006). However, little is known about their geodynamic setting, petrogenesis, and the information they may contain on crustal accretion in general and NCC development in particular. In this study, we present zircon geochronology, zircon Hf isotope data and whole rock trace element and Nd isotope compositions for TTG and TTG-like gneisses and associated amphibolites from the Taihua complex in the Lushan area of the southern NCC (1) to document the emplacement ages of these rocks, (2) to study their magma sources and petrogenetic processes, and (3) to discuss their tectonic significance for the southern NCC during the late Archean.

2. Geological background and samples

The North China Craton (NCC) can be divided into the Eastern and Western Blocks separated by the Trans-North China orogenic Belt (Fig. 1) on the basis of lithological, structural, metamorphic and geochronological differences (Zhao et al., 2000, 2001, 2002). The Western Block can be subdivided into southern and northern parts (Zhao et al., 2005). The late Archean basement of the eastern and western blocks is dominated by Late Archean TTG gneiss domes surrounded by minor supracrustal rocks (Zhao et al., 2005). The latter underwent greenschist to granulite facies metamorphism at ~2.5 Ga and were also affected by a ~1.85 Ga metamorphic event (Zhao et al., 2000, 2005). The Trans-North China Orogen represents a collision event between the two blocks at ~1.85 Ga (Zhao et al., 2000, 2001, 2002).

The Taihua Group, a suite of early Precambrian medium-high grade metamorphic rocks consisting of greenstone belts and a series of graphite-bearing gneisses, biotite gneisses, marbles and banded iron formations, crops out in several terranes distributed along the southern margin of the NCC (Fig. 1a). These metamorphic rocks have been further subdivided into the Paleoproterozoic Upper Taihua and Late Archean Lower Taihua Groups according to supracrustal rock types (Zhang et al., 1985; Kröner et al., 1988; Xue et al., 1995; Tu, 1998; Wan et al., 2006). The Lower Taihua Group is mainly composed of amphibolites and gneisses. The Upper Taihua Group unconformably overlies the Lower Taihua Group, and is dominated by graphite-bearing gneisses, biotite gneisses, marbles, banded iron formations and amphibolites (Tu, 1998; Wan et al., 2006).

In the Lushan area, the Taihua Group extends in a northwest-southeast direction in fault or unconformable contact with the Mesoproterozoic Ruyang Group and Cambrian cover in the northeast (Fig. 1b). In the southwest, the Mesoproterozoic Xionger Group shows an unconformable contact (Fig. 1b) with Upper Taihua Group. Amphibolites of Lower Taihua Group occur as enclaves (<~100 m in length) in the widespread Archean grey gneisses (~60–70% of the exposed rocks; Zhang et al., 1985) and locally show "being intruded by the gneisses" probably prior to the major phase of regional metamorphism/deformation because the foliation in the gneisses parallel to the elongation of the amphibolite enclaves and the light veins at the edge of amphibolite (Fig. 2a–d). The gneisses show typical gneissic fabrics with parallel layering and alignment of plagioclase with amphiboles or biotites (Fig. 2b–d). Furthermore, the gneisses can be readily subdivided into dark-grey and light-grey suites according to color and intrusive relationship (Fig. 2a and b). The light-grey gneisses always show relationships of (1) intruding the dark-grey gneisses and amphibolites (Fig. 2a and b), (2) concordant gneissic foliation with the dark-grey suite, yet (3) irregular contact with amphibolites (Fig. 2a–d). The dark-grey gneisses can be readily distinguished from amphibolites by gneissic foliation in the gneisses that parallels the elongation of the amphibolite enclaves. In some locations (e.g., northern part of Lushan area, such as Beizi in Fig. 1b), both dark-grey and light-grey gneisses are also interlayered with amphibolites because of strong foliation (Fig. 2e). In general, dark-grey gneisses mostly occur in the northern area, while light-grey gneisses mostly occur in the southern area (Fig. 1b). To avoid the probable effects of alteration and weathering on the geochemistry, we collected fresh samples for this study from central portions of each lithology away from lithological contacts and regions with strong foliation.

Amphibolites are dominated by amphibole (50–90%) with subordinate plagioclase (5–30%), clinopyroxene (<10%) and garnet (<10%). The light-grey gneisses consist of plagioclase (50–55%), quartz (25–30%), biotite (10–15%), amphibole (<10%), clinopyroxene (<3%) and K-feldspar (<5%). The mineral assemblage of dark-grey gneisses includes plagioclase (40–50%), amphibole (10–30%), clinopyroxene (<10%) and biotite (<5%). Sphene, magnetite and apatite are the common accessory minerals (<1%). All these three rock types show granoblastic and "triple junction" textures. Grey gneisses show layering defined by mineral mode variation.

3. Analytical methods

Bulk-rock geochemical and Nd isotopic analyses were done at the Guangzhou Institute of Geochemistry, Chinese Academy of Sciences (GIG-CAS). Major elements were determined using standard X-ray fluorescence (XRF) technique on a Rigaku ZSX100e following Li et al. (2006). Analytical uncertainties of all major elements are between 1% and 5%. Trace elements were analyzed using induc-

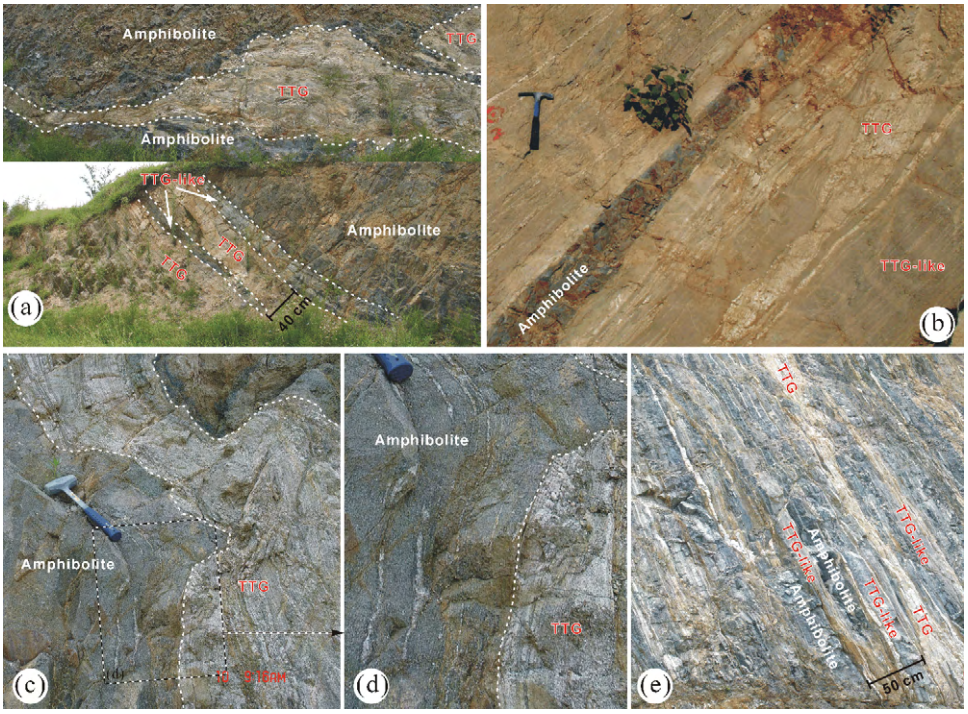

Fig. 2. Field photographs: (a) light-grey felsic TTG gneisses (TTG) irregularly intruded amphibolite but in concordance with dark-grey gneisses (TTG-like) with distinct interface, while TTG-like rocks gradually changes to amphibolite; (b) amphibolites "interlayered" within the widely distributed gneisses; TTG gneisses intruded into TTG-like gneisses and developed concordant gneissic foliation; (c and d) The TTG gneisses "intruded" amphibolite as ptygmatic folds, and show typical gneissic fabrics with parallel layering and alignment of plagioclase with amphiboles or biotites; some felsic dikelets in amphibolites parallel to the fabrics of the TTG gneisses; (e) the interlayered TTG-like gneisses, TTG gneisses and amphibolites in a strongly foliated zone.

tively coupled plasma-mass spectrometry (ICP-MS) following Li (1997). Precision for REE and other incompatible elements is estimated to be better than 5% on the basis of repeated analysis of USGS reference rock standard BIR-1 and laboratory standard (ROA-1). Within-run analytical precision for Nd is better than 2.5% RSD (relative standard deviation). The Sm/Nd ratios measured by ICP-MS are within 2% uncertainty (Li et al., 2002), and calculation of $\varepsilon_{Nd}(t)$ values for samples of the present study using these Sm/Nd ratios results in uncertainties less than 0.25 units, which is negligible for our petrogenetic discussion. Nd isotopic analyses were done on a Micromass Isoprobe multi-collector ICP-MS following Li et al. (2004). Reference standards analyzed along with samples give $^{143}Nd/^{144}Nd = 0.512124 \pm 11$ (2σ) for Shin Etsu JNdi-1 (0.512115 ± 7; Tanaka et al., 2000).

Zircons were extracted using a combined technique of heavy liquid and magnetic separation followed by hand-picking under a binocular microscope. They were mounted together with a zircon standard (TEMORA) in epoxy resin. The mount was polished to ensure grain exposure before gold-coating. The internal structure of zircons was examined using cathodoluminescence (CL) prior to U–Pb isotopic analyses. The U–Pb analyses were done mainly using a Sensitive High-Resolution Ion Microprobe (SHRIMP II) at the Beijing SHRIMP Center (in the Institute of Geology, Chinese Academy of Geological Sciences, Beijing). The analytical procedures are similar to those described by Williams (1998). The zircon standard TEMORA (age 417 Ma) of RSES was used to correct for inter-element fractionation. U, Th and Pb concentrations were determined based on the standard Sri Lankan gem zircon SL13, which has 238 ppm U and an age of 572 Ma. Squid (ver. 1.04) and Isoplot (ver. 3.23) software were used for data reduction and age calculation with ^{204}Pb-based method of common Pb correction applied. Uncertainties reported in Supplementary Table 1 are expressed in terms of $\pm 1\sigma$ from the means. The ages quoted in the text ($^{207}Pb/^{206}Pb$ ages) are the weighted means at the 95% confidence level.

In situ zircon Hf isotopic analyses were done on dated spots using a Neptune MC-ICPMS, equipped with a 193 nm laser, at the Institute of Geology and Geophysics, Chinese Academy of Sciences in Beijing (IGG-CAS). Spot sizes of 40 μm with a laser repetition rate of 8 Hz at 100 mJ were used. The detailed analytical technique and data correction procedure are described in Xu et al. (2004) and Wu et al. (2006) During the analysis of our unknown samples, the zircon standard (91500) gave $^{176}Hf/^{177}Hf = 0.282292 \pm 14$ (2σ) and $^{176}Lu/^{177}Hf = 0.00029$, similar to the $^{176}Hf/^{177}Hf$ ratios of 0.282284 ± 22 measured using the LA-MC-ICPMS method (Griffin et al., 2006).

4. Results

4.1. Zircon U–Pb geochronology and Hf isotopes

4.1.1. Zircon SHRIMP U–Pb dating

Zircons from a more mafic sample of dark-grey gneisses (TH05-2) are mostly fragmented or slightly rounded crystals (Fig. 3a). CL images of most zircons show oscillatory zonings in the cores (Fig. 3a) pointing to a magmatic origin, but the rims have no obvious oscillatory zonings. These morphological characteristics are likely caused by metamorphism and deformation. Except for Spots 8.1 and 10.1 containing very low Th, all other analyses show high Th/U ratios (0.34–1.41) (see Supplementary Table 1), which are consistent with a magmatic origin. Most analyses give similar $^{207}Pb/^{206}Pb$ ages (2690 ± 27 to 2767 ± 8 Ma), but varied $^{206}Pb/^{238}U$ ages (2211 ± 39 to 2809 ± 35 Ma) (Supplementary Table 1). A regression line of these analyses ($n = 13$; except for Spots 4.1 and 14.1) yields an upper intercept age of 2765 ± 13 Ma (MSWD = 1.3) (Fig. 3a), which is interpreted as formation age of the protolith of dark-grey gneisses. Two analyses (Spots 4.1 and 14.1) have a younger $^{207}Pb/^{206}Pb$ age of 2142–2190 Ma, which may be associated with magmatic event of the Upper Taihua Group (Wan et al., 2006).

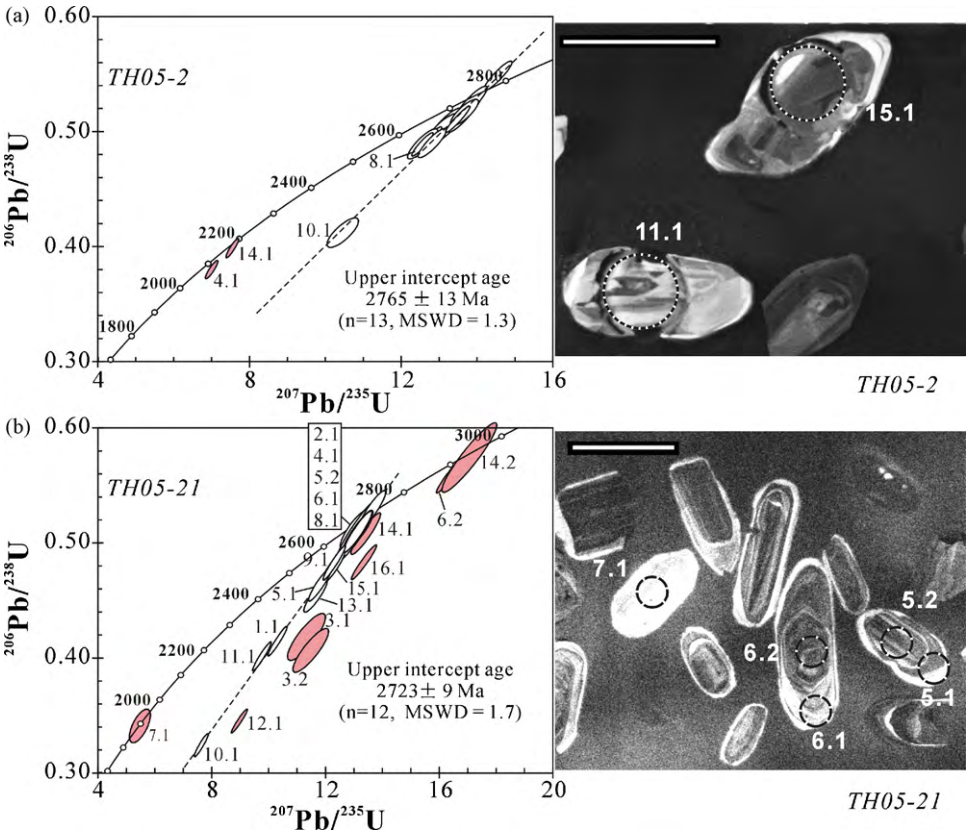

Fig. 3. Concordia diagrams for zircon SHRIMP U–Pb chronology of the Lushan gneisses and representative CL images of zircons. The circles indicate dating spots (30 μm diameter) and laser ablation for in situ zircon Hf isotopic analyses (40–50 μm diameter). The scale bar is 100 μm.

Zircons from an intermediate sample of light-grey gneisses (TH05-21) are mostly euhedral, sub-euhedral and slightly rounded (Fig. 3b). CL images show that these zircons are dominated by simple oscillatory zoning of magmatic origin. Most of them (Spots 1.1, 2.1, 4.1, 9.1, 10.1, 11.1, 13.1 and 15.1) gave relatively similar $^{207}Pb/^{206}Pb$ ages (2574 ± 7 to 2718 ± 10 Ma) but varied $^{206}Pb/^{238}U$ ages (1809 ± 20 to 2737 ± 28 Ma) (Supplementary Table 1), defining a linear array on the concordia diagram (Fig. 3b). A few zircons show clear cores and rims (Spots 3.1, 3.2, 5.1, 5.2, 6.1, 6.2, 8.1, 14.1 and 14.2; Fig. 3b). The cores commonly show micro-scale oscillatory zoning, suggesting a magmatic origin, which are likely inherited relic zircons with a wide range of $^{207}Pb/^{206}Pb$ ages (2698 ± 8 to 2946 ± 14 Ma; see Supplementary Table 1). The rims show another episode of magmatic oscillatory zoning (Spots 3.1 5.1, 6.1, 8.1 and 14.1), and mostly vary in a linear array defined by simple magmatic zircons (Fig. 3b). Regression of the analyses in the linear array (n = 12; Spots 1.1, 2.1, 4.1, 5.1, 5.2, 6.1, 8.1, 9.1, 10.1, 11.1, 13.1 and 15.1) yields an upper intercept age of 2723 ± 9 Ma (MSWD = 1.7) (Fig. 3b), which is interpreted as magmatic age of the light-grey gneisses. The analysis of Spot 7.1 has a young age (~1.9 Ga) similar to metamorphic recrystallization age of lower crust beneath the southern NCC (Huang et al., 2004).

4.1.2. LA-ICPMS Lu-Hf isotopes

Most zircons for Lu-Hf analyses have been dated by SHRIMP U–Pb methods on the same spots, and Lu-Hf isotopic results are listed in Supplementary Table 2. The initial Hf isotope ratios are all calculated at the dated ages of the magmatism. Zircon $\varepsilon_{Hf}(t)$ values of TH05-21 are slight higher than those of TH05-2 (Fig. 4a). Additionally, single-stage primitive mantle Hf model ages for zircons of TH05-21 are slightly younger than those of TH05-2 (Fig. 4b). As a whole, the inherited zircons in TH05-21 have similar $\varepsilon_{Hf}(t)$ values to those of other zircons, but $\varepsilon_{Hf}(t_2)$ values are high when calculated using their $^{207}Pb/^{206}Pb$ ages (Fig. 4c) (see Supplementary Table 2), some of which are very close to the value on the evolution curve of the depleted mantle (Griffin et al., 2000) (Fig. 4c).

4.2. Major and trace elements

The amphibolites contain low-SiO_2 (44.4–49.6 wt%), high-MgO (4.99–8.12 wt%), Fe_2O_3 (7.97–17.8 wt%), TiO_2 (0.40–1.57 wt%) and CaO (9.80–15.8 wt%). The grey gneisses have high SiO_2 (52.3–74.3 wt%) and Na_2O (3.75–6.48 wt%) but relatively low-MgO, Fe_2O_3, TiO_2 and CaO (Supplementary Table 3). In the triangle diagram of normative feldspar composition, our samples vary from tonalite, trondhjemite to granite, and most grey gneisses plot in the field of tonalite (Fig. 5). From amphibolite to dark-grey and to light-grey gneisses, TiO_2, Fe_2O_3, MgO, MnO and CaO decrease with increasing SiO_2 (Fig. 6). Both amphibolites and light-grey gneisses have a large range of Al_2O_3 negatively correlated with SiO_2, but dark-grey gneisses have relatively constant Al_2O_3 (Fig. 6e).

The amphibolites show flat REE patterns ($[La/Yb]_N$ = 0.8–3.4) without obvious Eu anomalies (Fig. 7a). On the primitive mantle-normalized multi-element spidergram, amphibolites show nearly flat patterns but have weak negative Ta–Nb and P anomalies, a positive Pb anomaly and variable Th and U (Fig. 7b). The gneisses all show LREE-enriched and HREE-depleted patterns. The dark-grey gneisses have low HREE (Yb_N = 3.0–5.4) and Y (8.07–13.9 ppm) with moderate to high $[La/Yb]_N$ (6.7–37.1) and Sr/Y (25.9–119.3), and show moderate negative to weak positive Eu anomalies (0.76–1.04; see Supplementary Table 3). The light-grey gneisses have very low REE (Yb_N < 1.8) and Y (<4 ppm) with a wide range of $[La/Yb]_N$ (5.2–86.6), Sr/Y (71.4–949), showing obvious positive Eu anomalies (1.20–2.43; see Supplementary Table 3). On the primitive mantle-

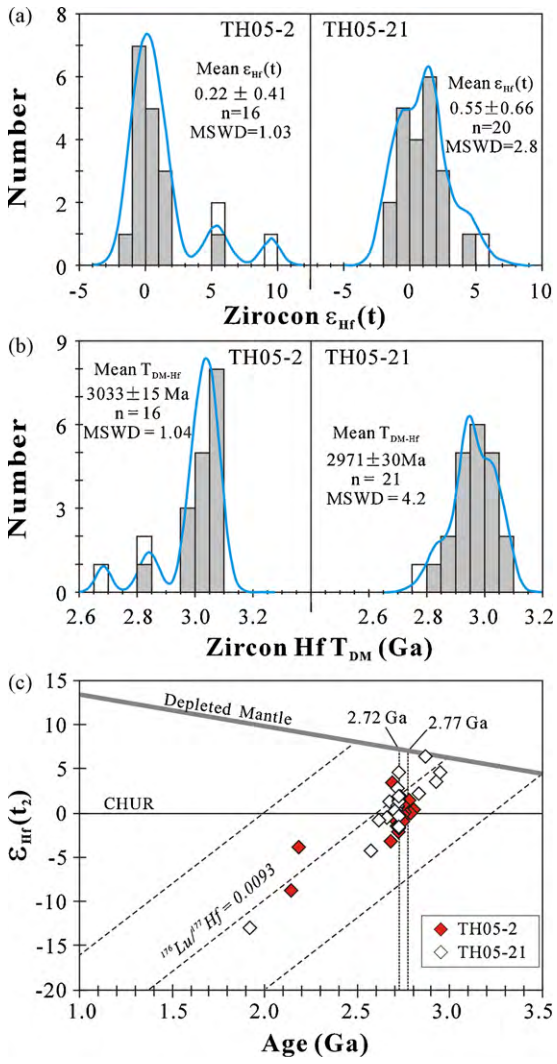

Fig. 4. Initial Hf isotope ratio and Hf model ages for zircons from gneisses of the Lower Taihua group. (a) Histograms of initial zircon $\varepsilon_{Hf}(t)$, t = 2.77 Ga for TH05-2 and 2.72 Ga for TH05-21; (b) histograms of single-stage depleted mantle zircon Hf model ages; (c) diagram of Hf isotope evolution; t_2 are $^{207}Pb/^{206}Pb$ ages by SHRIMP U–Pb dating (Supplementary Table 1); the evolution of depleted mantle (DM) is drawn by using a present-day $^{176}Hf/^{177}Hf = 0.28325$ and $^{176}Lu/^{177}Hf = 0.0384$ (Griffin et al., 2000).

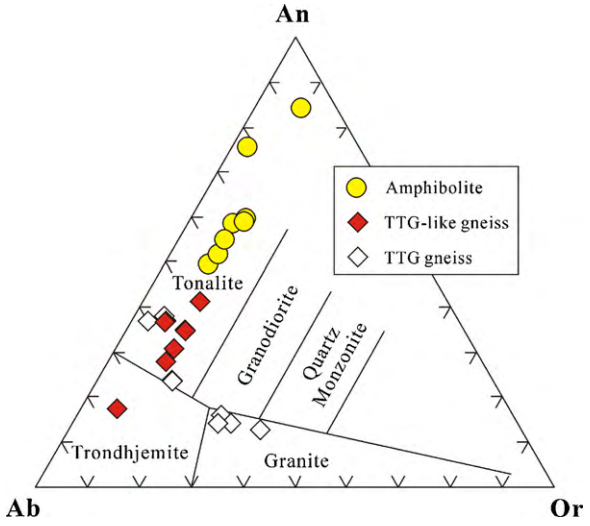

Fig. 5. Normative feldspar composition for amphibolites and gneisses of the Lushan lower Taihua group in An–Ab–Or classification diagram (Barker, 1979).

normalized spidergram, the dark-grey gneisses are characterized by enrichment of Rb, Ba, K and LREE and pronounced negative Nb–Ta, P and Ti anomalies (Fig. 7d), while the light-grey gneisses show negative Nb–Ta–Ti but positive Sr and Pb anomalies and depletion of Th, U and HREE (Fig. 7d).

Alkalis, particularly K, Rb and Cs, are mobile and often lost during high grade metamorphism. The degree of alkali loss can be estimated roughly by the concentration of Rb and the K/Rb ratio (Fig. 8) (Jahn and Zhang, 1984). Variable Rb depletion relative to K follows the trend defined by the Archean granulites from the eastern NCC (Huang et al., 2004), and nearly all data points have ratios much higher than the main trend defined by Shaw (1968) for continental igneous rocks and the average basaltic to felsic rocks in Archean greenstone belts (Jahn and Zhang, 1984). The higher than normal K/Rb ratios of the Lushan samples suggest that Rb is preferentially lost relative to K. It is also very important to examine if other elements (such as Na_2O, Sr, Ba and REEs) may have been modified by the metamorphism. If so, the degree of modification could be related to the degree of Rb loss which is highly variable. It is observed that similar REE patterns of the same suite of rocks have very different Rb concentrations and K/Rb ratios. This implies that the REE patterns have not changed while alkalis may have during metamorphism. MORB-like REE patterns of the amphibolites (Fig. 7a) suggest that REE and Y may indeed reflect the primary characteristics of the protoliths. The Lushan amphibolites and gneisses all show good relationship between Na_2O and SiO_2 (Fig. 6h), indicating that Na_2O may not have been significantly affected by metamorphism. Sr is known to be less mobile than Rb during alteration and metamorphism mostly because of the buffering effect of plagioclase in which Sr is compatible. Other elements like Pb and U are readily mobile during metamorphism.

All the gneiss samples plot in the field of adakite and high-Al TTG on $[La/Yb]_N$ versus Yb_N and Sr/Y versus Y diagrams (Fig. 9), but dark-grey gneisses and light-grey gneisses show two different trends because of different Y and HREE abundances. As a whole, the light-grey gneisses resemble TTGs with high SiO_2 (>64 wt%), high Na_2O (3.75–5.01 wt%) and low ferromagnesian elements (e.g., $Fe_2O_3 + MgO + MnO + TiO_2 < 5$ wt%, with an average $Mg^{\#}$ of 0.43 and average Ni and Cr contents of 14 and 29 ppm, respectively) (Martin et al., 2005). We thus call these light-grey gneisses as TTGs or TTG gneisses for discussion convenience. Some TTG samples have relatively high K_2O (3.06–3.93 wt%; see Supplementary Table 3) due to their K-feldspar rich nature as a result of greater extent of fractional crystallization and/or repeated re-melting. We call the dark-grey gneisses as "TTG-like" or TTG-like gneisses for discussion convenience (Fig. 9) as they are not typical TTG (Martin et al., 2005) for its low-SiO_2 (52.4–66.1 wt%) and high ferromagnesian ($Fe_2O_3 + MgO + MnO + TiO_2$ = 4.68–15.9 wt%, $Mg^{\#}$ = 0.47–0.68, Ni = 13.1–77.2 ppm, Cr = 17.5–130 ppm; see Supplementary Table 3). The dark-grey gneisses are compositionally dioritic rock but not sanukitoid ($Mg^{\#} > 0.6$; Ni > 100 ppm; Cr = 200–500 ppm; $Ce_N > 100$; $[Ce/Yb]_N$ = 10–50; Shirey and Hanson, 1984).

4.3. Nd isotope

Nd isotope compositions of Lushan TTG and TTG-like gneisses and amphibolite are listed in Supplementary Table 4. Whole rock $^{143}Nd/^{144}Nd$ ratios of the amphibolite samples are relative higher (0.511402–0.513272) than those of the gneiss samples (0.510238–0.511336). The amphibolites and TTG-like gneisses all have positive $\varepsilon_{Nd}(t)$ (0.26–3.25), whereas TTG gneisses have relatively low $\varepsilon_{Nd}(t)$ (−1.31 to −0.23). As a whole, $\varepsilon_{Nd}(t)$ decreases from amphibolites to TTG-like gneisses and to TTG gneisses (Fig. 10a). Single-stage Nd model ages (T_{DM}) of amphibolites vary significantly (1915–4956 Ma) because of variable $f_{Sm/Nd}$ (−0.38–0.13), but con-

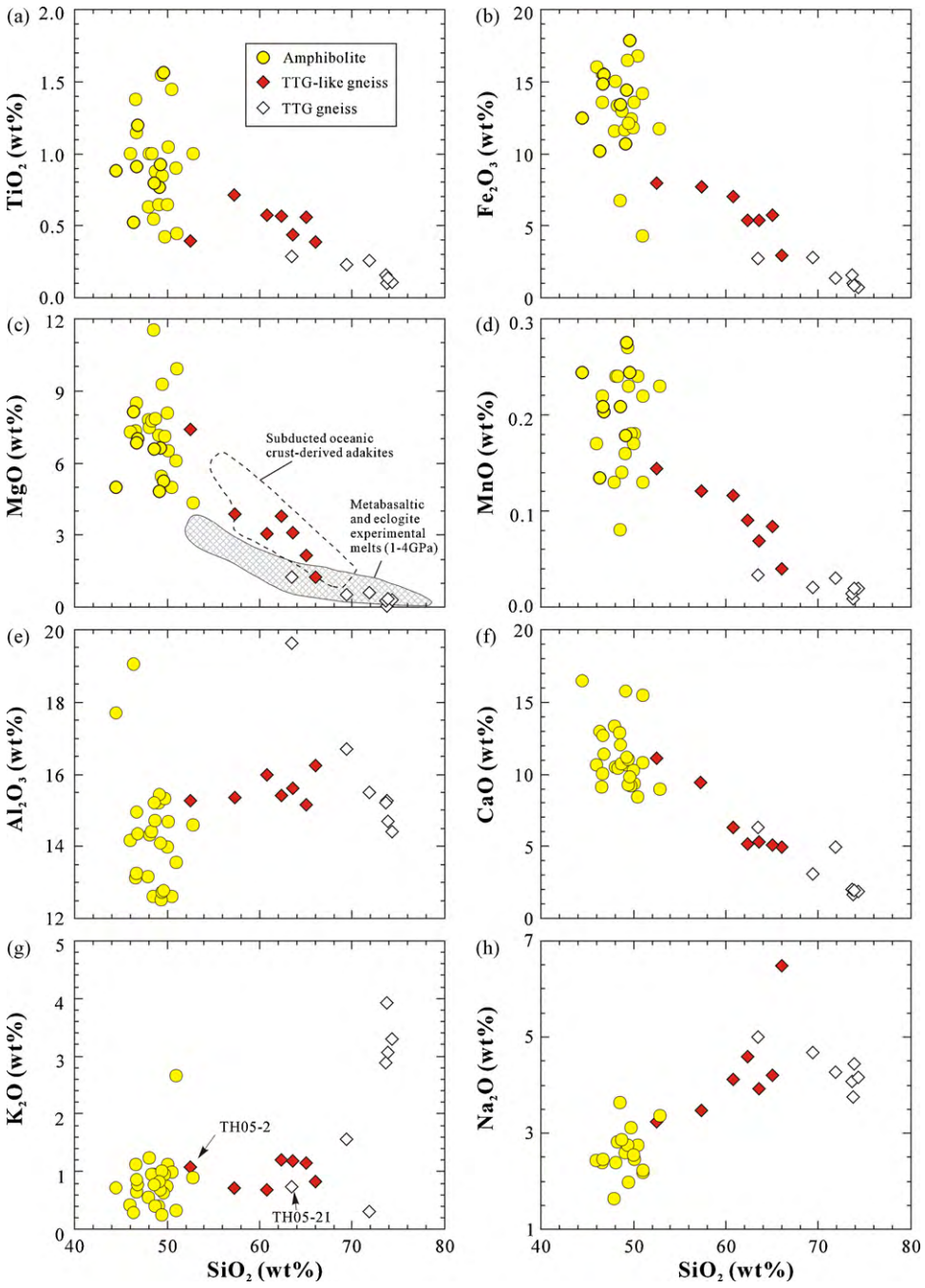

Fig. 6. SiO_2 variation diagrams of representative major element oxides for amphibolites and gneisses from the Lushan lower Taihua group. Some amphibolite data are from Xue et al. (1995). Fields of subducted oceanic crust-derived adakites and metabasaltic and eclogite experimental melts are after the compilations of Wang et al. (2006).

centrate in the range of 2837–3025 Ma if we exclude three samples (TH05-10, TH05-22 and B-20) with high $f_{Sm/Nd}$ which could be caused by strong alteration (LOI > 3% in B-20; Xue et al., 1995) or nonuniform distribution of garnet (high Al_2O_3 contents in TH05-10, TH05-22). Single-stage Nd model ages of TTG-like and TTG gneisses vary in a range of 2981–3012 and 3033–3112 Ma, respectively (see Supplementary Table 4).

Nd isotopes of Lushan Lower Taihua complex differ significantly from the late Archean rocks of the Eastern Block (e.g., Eastern Hebei and Taishan of Western Shandong; Jahn et al., 1988; Yang et al., 2008) and North part of Trans-North China Orogenic belt (e.g., Zhongtiaoshan and Wutaishan-Fupin; Sun et al., 1992; Sun and Hu, 1993) or the early Archean rocks from Qianan of Eastern Hebei (Huang et al., 1986; Jahn et al., 1987). The integrated Lushan lower Taihua complex was originally derived from depleted mantle at 2.8–3.1 Ga (Fig. 10b).

5. Discussion

5.1. Petrogenesis of the Lushan gneisses

The Lushan gneisses all have high Sr/Y and La/Yb ratios characteristic of TTGs and adakites (Martin et al., 2005; Condie, 2005). Such signature could result from melting of a high Sr/Y source (Moyen, 2009) or from different contributions of plagioclase, amphibole or garnet during melting (e.g., Martin et al., 2005; Moyen, 2009). The Lushan TTG and TTG-like gneisses are products of two different events as revealed by field relationships (Fig. 2b)

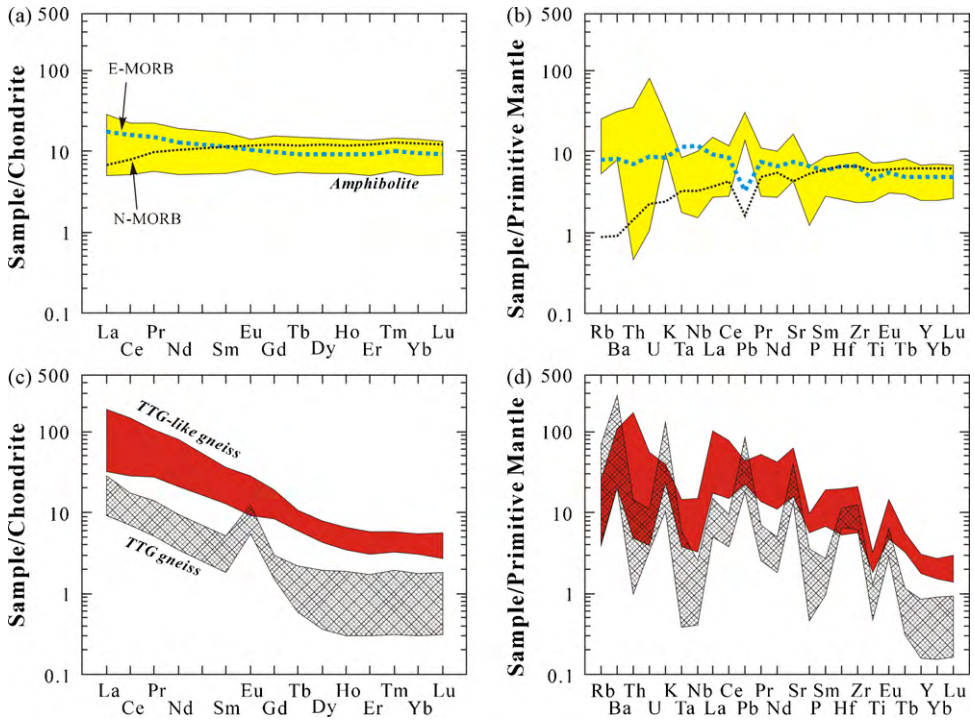

Fig. 7. Chondrite-normalized REE patterns and primitive mantle-normalized trace-element spidergrams for amphibolites (a and b) and gneisses (c and d) from the Lushan lower Taihua group. Chondrite and PM normalization factors are from Taylor and McLennan (1985) and Sun and McDonough (1989), respectively; N-MORB and E-MORB from Sun and McDonough (1989).

and age differences (Fig. 3). The Lushan TTG gneisses obviously have much more complex sources than the TTG-like gneisses from their high proportion of inherited zircons (Fig. 3b) and relatively low $\varepsilon_{Nd}(t)$ values (Supplementary Table 4). In addition, the TTG-like gneisses occur mostly in the northern Lushan area, while the TTG gneisses are more abundant in the southern Lushan area. Thus, it is less likely that the protolith of the TTG gneisses could be partial melts of the TTG-like gneisses.

Melting of a high Sr/Y and La/Yb source is possible, but is unlikely for the petrogenesis of the TTG-like gneisses because there is no evidence for the presence of such an Archean source rock in the southern NCC. High Sr/Y and La/Yb ratios in the Lushan TTG-like gneisses are likely due to different roles of plagioclase, amphibole or garnet. Plagioclase fractionation can effectively reduce Sr, Sr/Y and Eu/Eu*. Relatively low Eu/Eu* (Supplementary Table 3; Fig. 11a and b) in two TTG-like gneiss samples is consistent with a weak plagioclase modal deficiency in the rock. Sr/Y and La/Yb in the melt could increase significantly as a result of fractionation of amphibole and/or garnet at relatively high pressures or partial melting with residual amphibole and/or garnet (Castillo et al., 1999), but this would also lead to SiO_2 increase (Macpherson et al., 2006), yet the lack of Sr/Y (and La/Yb) correlation with SiO_2 for the TTG-like gneisses (Supplementary Table 3) suggests that the high Sr/Y and La/Yb in these rocks are not due to amphibole and/or garnet fractionation.

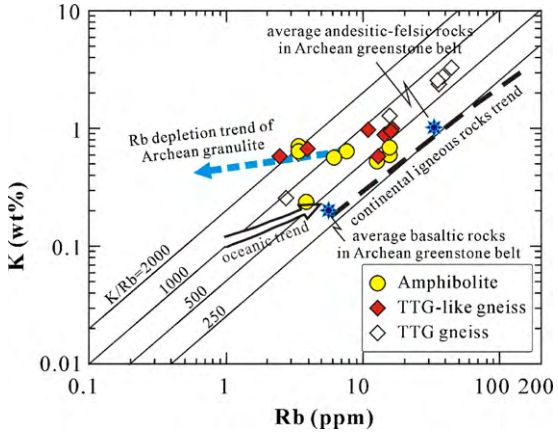

Fig. 8. K vs. Rb diagram for the Lushan amphibolites and gneisses. Rb depletion trend of Archean granulites of eastern North China Craton based on Huang et al. (2004), trends for continental igneous rocks and oceanic tholeiites from Shaw (1968), and the average basaltic to felsic rocks in Archean greenstone belts from Jahn and Zhang (1984).

Furthermore, amphibole has a high K_D for HREEs, but even higher for medium to heavy REEs (e.g., Dy); therefore, amphibole removal can induce decreasing Dy/Yb ratios. Although amphibole fractionation is commonly accompanied by plagioclase removal in natural systems, the net effect of amphibole and plagioclase fractionation is an increase in La/Yb, decrease in Dy/Yb, and moderate increase or even decrease in Sr/Y (Moyen, 2009). The Lushan TTG-like gneisses show a positive correlation between Sr/Y and La/Yb, and Dy/Yb increases with increasing Sr/Y and to a lesser extent La/Yb (Fig. 12b and c). Thus fractionation of amphibole and plagioclase may be involved, but cannot thoroughly explain the high Sr/Y and La/Yb ratios of the Lushan TTG-like gneisses. Unlike amphibole, garnet fractionation will not only effectively raise the Sr/Y and La/Yb ratios, but also increase the Dy/Yb ratio in the melt (Fig. 12) (Macpherson et al., 2006; Davidson et al., 2007). Because garnet is also an aluminous mineral, its fractionation will also reduce Al_2O_3 with increasing SiO_2 in the residual melts. Relatively constant Al_2O_3 in the Lushan TTG-like gneisses (Fig. 6e) is again inconsistent with garnet fractionation. All these signatures, however, are qualitatively consistent with partial melting with garnet as a residual phase. Thus partial melting with residual amphibole and/or garnet can better explain the high Sr/Y and La/Yb ratios in the Lushan TTG-like gneisses. In general, partial melting of mafic rocks with a residue of eclogite or amphibole-bearing eclogite would produce TTG (Martin et al., 2005; Condie, 2005). However, it is

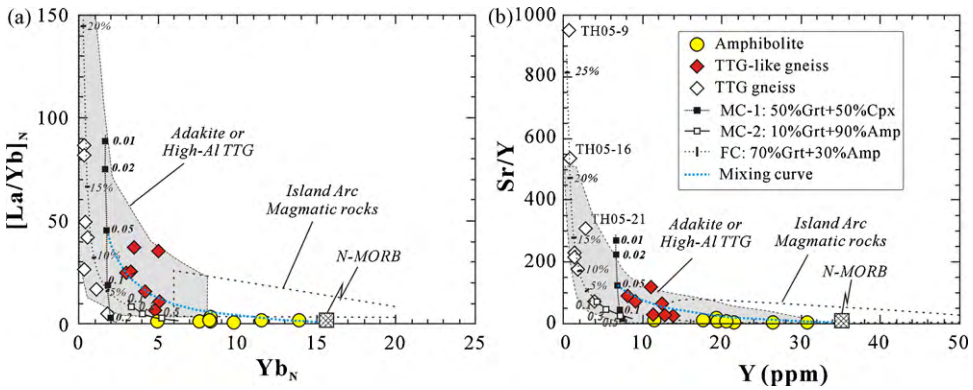

Fig. 9. Plots of $(La/Yb)_N$ vs. Yb_N and Sr/Y vs. Y for the amphibolites and gneisses from the Lushan lower Taihua group. Fields of high-Al TTG, adakite and common island arc magmatic rocks are from Defant and Drummond (1990) and Martin et al. (2005). MC-1: fractional melting curve of N-MORB; MC-2: fractional melting curve of "30% lower crust + 70% N-MORB"; FC: Rayleigh fractionation curve of 10% melts on MC-2; Mixing curve: between N-MORB and 5% melts on MC-1. Partition coefficients in the system of andesitic to tonalitic melts were used in the calculation: amphibole (Sisson, 1994), garnet and clinopyroxene (Barth et al., 2002). The N-MORB average from Hofmann (1988) and lower crust from Rudnick and Gao (2003).

unlikely that the Lushan TTG-like gneisses were formed by partial melting of an oceanic crust alone, which would require a rather high-degree partial melting for its low-SiO_2 and high-MgO contents. The characteristics of low-SiO_2 and high mafic elements in the Lushan TTG-like rocks suggest the participation of some mafic melts. Archean sanukitoid with low-SiO_2 and high mafic elements is most likely re-melting of peridotite previously metasomatised via addition of slab-melt (Shirey and Hanson, 1984; Martin et al., 2005). But this process is unlikely to be responsible for the Lushan TTG-like gneisses because of their low-$Mg^{\#}$, Cr and Ni relative to typical sanukitoids. The contamination of "TTG" by basaltic magmas may account for the genesis of the Lushan TTG-like magmas (Figs. 9 and 12), which can result in the high Sr/Y and La/Yb TTG-like magmas with high-MgO, Cr and Ni relative to typical TTG.

Notable positive Eu anomalies and the correlations between Sr, Sr/Y and Eu/Eu^* observed in the Lushan TTG gneisses (Fig. 11) are indicative of varying extent of plagioclase accumulation in the rock because plagioclase has excessively high positive Sr and Eu anomalies yet highly depleted in all other REEs with a characteristic $[La/Yb]_N > 1$ (McKay et al., 1994; Niu and O'Hara, 2009), which also explains the REE patterns of the TTG gneisses (Fig. 7c). The plagioclase accumulation may have been further diluted by quartz for its high SiO_2 and very low LREEs, which is evidenced by a negative relationship between Na_2O and SiO_2 (Fig. 6h). Amphibole and/or garnet fractionation or the presence of these minerals in the melting residue will also promote Sr/Y and La/Yb ratios in the Lushan TTG gneisses. The very high Sr/Y ratios and positive Eu anomalies in some TTG gneiss samples (TH05-21, TH05-16 and TH05-9) are most likely attributed to the plagioclase accumulation (Fig. 11), but high Sr/Y and La/Yb ratios of other samples are mostly elevated by the fractionation of garnet and/or amphibole because of good positive correlations between Sr/Y, $(La/Yb)_N$ and Dy/Yb (Fig. 12). High-pressure origin has become implicit in the term "Archaean TTG" because the features of high-Al TTG reflect the presence of garnet and amphibole as well as the lack of plagioclase either as residual or fractionating phases (Martin et al., 2005). It is very hard to evaluate the exact behavior of amphibole and garnet in the residue during partial melting, which had been diluted by the plagioclase accumulation and garnet ± amphibole fractionation. The plagioclase accumulation cannot explain the large variation of Dy/Yb, but partial melting with residual garnet will effectively raise the Dy/Yb ratios in the melt while residual amphibole will decrease Dy/Yb ratios. Thus the similar Dy/Yb between the less fractionation samples (TH08-10, TH05-21, TH05-16 and TH05-9) and the amphibolites (Fig. 12b) might indicate the effects of residual garnet-amphibolite. The negative $\varepsilon_{Nd}(t)$ values and a high proportion of inherited zircons in the Lushan TTG gneisses indicate that the source material for partial melting might contain some preexistent crustal materials.

In brief, the Lushan TTG and TTG-like gneisses have different origins. The TTG rocks resulted from crustal melting involving older materials, followed by garnet ± amphibole fractionation and

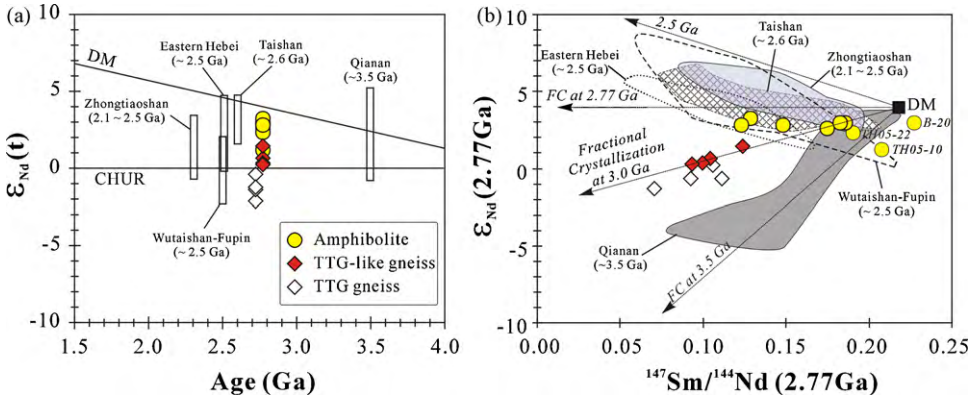

Fig. 10. Nd isotopic evolution diagrams for the Lushan amphibolites and gneisses: (a) $\varepsilon_{Nd}(t)$ vs. ages; (b) $\varepsilon_{Nd}(2.77\ Ga)$ vs. $^{147}Sm/^{144}Nd$. Some typical Archean rocks from North China Craton are also shown for comparison. Eastern Block: Qianan (EH) amphibolites (Jahn et al., 1987; Huang et al., 1986); Taishan (WS) amphibolites and grey gneisses (Jahn et al., 1988); Neoarchean intrusive rocks of eastern Hebei (EH) (Yang et al., 2008). Trans-North China Orogen: Wutaishan-Fupin (WT-FP) amphibolites and grey gneisses (Sun et al., 1992); Zhongtiaoshan (ZT) metamorphic basaltic rocks (Sun and Hu, 1993). Abbreviations of metamorphic complexes shown in Fig. 1a.

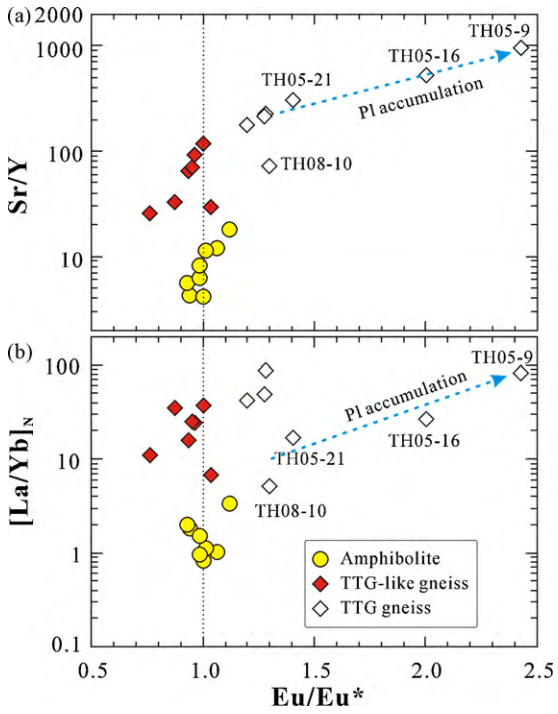

Fig. 11. Diagrams of Sr/Y, $[La/Yb]_N$ vs. Eu/Eu* for the Lushan amphibolites and gneisses.

plagioclase accumulation. The TTG-like rocks formed as a result of mixing between basaltic magmas and partial melts of mafic crust with residual amphibole or garnet or both.

5.2. Source characteristics of the Lushan gneisses

Subducting ocean crust under eclogite facies condition would be the potential source material for TTGs as an Archean analogue of Cenozoic adakite (Defant and Drummond, 1990; Drummond et al., 1996; Kay et al., 1993; Martin, 1999; Martin et al., 2005). However, most early Archean and many late Archean TTG suites are not analogues of Cenozoic adakite, but more likely represent partial melts of basaltic lower crust rather than of subducted/subducting ocean crust (Smithies and Champion, 2000; Smithies, 2000; Condie, 2005). Therefore, careful geochemical evaluations are needed in ascertaining source materials of the Archean TTGs.

Partial melts of the subducting ocean crust will interact with peridotitic mantle during ascent, resulting in high-MgO, Cr and Ni contents (Smithies, 2000; Martin et al., 2005; Moyen, 2009). The Lushan TTG-like gneisses have low-SiO_2 and high-MgO (or $Mg^{\#}$), Cr and Ni relative to typical TTG, which is consistent with the model of partial melts of peridotitic mantle interaction with partial melts of a subducting ocean crust (Fig. 6c, 13a and b). Positive $\varepsilon_{Nd}(t)$ values without relic zircons in the Lushan TTG-like gneisses is also consistent with the slab melting model. Additionally, whole rock Nd model ages of the TTG-like gneisses (based on depleted mantle) are very close to the zircon Hf model ages ~3033 ± 15 Ma (Fig. 4b; Supplementary Table 2). Because zircon is a mineral rich in Hf with very low Lu, its fractionation from magma can result in the preferential retention of Lu over Hf in the residual melt. Therefore any pre-fractionation of zircons from the system or participation of ancient crust into the system would cause differences in Nd–Hf variation (Huang et al., 2009). So the matching zircon Hf and bulk-rock Nd model ages indicate that there is no obvious pre-fractionation of zircons from the system or participation of pre-existing crustal materials in the generation of the Lushan TTG-like rocks.

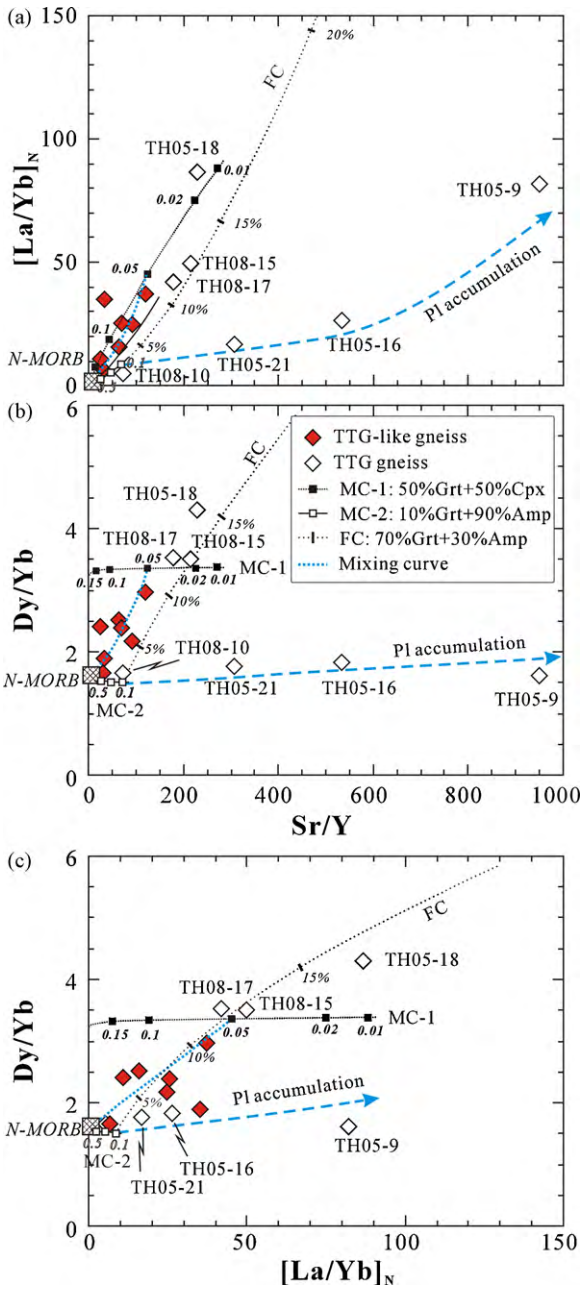

Fig. 12. Diagrams showing relationships between $(La/Yb)_N$, Sr/Y and Dy/Yb for the Lushan gneisses. Fractional melting curves (MC-1, MC-2), Rayleigh fractionation curve (FC) and mixing curve were calculated as shown in Fig. 9.

In contrast, the negative $\varepsilon_{Nd}(t)$ values in the Lushan TTG samples are similar to those of the thickened lower crust-derived melts, which is also consistent with the low-MgO (0.88–2.14 wt.%), Cr (5.21–31.1 ppm), Ni (1.64–11.6 ppm) and high SiO_2 (63.9–69.7 wt.%) in these samples (Fig. 13; Supplementary Table 3). Zircon Hf isotopes place further constraints on the nature of the source of the Lushan TTG. As a whole, positive average $\varepsilon_{Hf}(t)$ value (0.55 ± 0.66; Fig. 4a) in zircons from TH05-21 indicates the involvement of mantle-derived components in their petrogenesis. As most $\varepsilon_{Hf}(t)$ values of TH05-21 at 2.72 Ga are distinctively lower than that of the depleted mantle (Fig. 4c), the immediate source is likely a preexistent crustal material as evidenced by the presence of a high proportion of inherited zircons. The high $\varepsilon_{Hf}(t)$ values calculated for respective $^{207}Pb/^{206}Pb$ ages of some inherited zircons in TH05-21 are very close to the evolution curve of the depleted man-

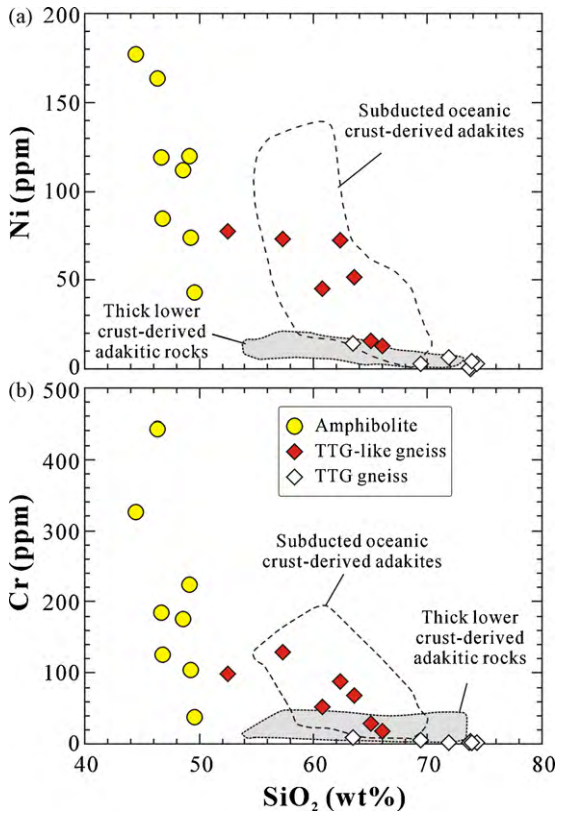

Fig. 13. Plots of (a) Ni vs. SiO_2 and (b) Cr vs. SiO_2 for the Lushan gneisses and amphibolites. Fields of adakites are after the compilations of Wang et al. (2006).

tle (Griffin et al., 2000) (Fig. 4c). We thus propose that the Lushan TTG were generated by partial melting of a crust formed during 2.95–2.80 Ga based on the $^{207}Pb/^{206}Pb$ ages of the relic zircons in TH05-21.

The Lushan gneiss samples all exhibit strong depletion of Nb, Ta and Ti on the primitive mantle-normalized trace-element spidergram (Fig. 7d). This behavior is generally interpreted as the effect of rutile or Ti-bearing amphibole crystallization or as residual phases in the source region (e.g., Ionov and Hofmann, 1995; Tiepolo et al., 2000, 2001; Coltorti et al., 2007; Foley et al., 1987; Klemme et al., 2005, 2006; Xiong et al., 2005). Amphibole removal could decrease Dy/Yb, and also lower the Nb/Ta but increase the Zr/Sm in the residue (Fig. 14a) (Tiepolo et al., 2000, 2001; Foley et al., 2002). Thus the strong negative correlation of Zr/Sm vs. Dy/Yb (Fig. 14b) and positive correlation of Nb/Ta vs. Dy/Yb (Fig. 14c) are indicative of amphibole as a residual phase during partial melting of ocean crust, which is consistent with the relatively flat HREE patterns (Fig. 7c) of the TTG-like rocks. However, the strong negative correlation between Dy/Yb and Ti/Ti* ($=2Ti_{PM}/[Sm_{PM}+Tb_{PM}]$) (Fig. 14d) and positive correlation between Zr/Sm and Ti/Ti* (Fig. 14e) suggests that amphibole removal might not be totally responsible for the strong depletion of Nb–Ta–Ti in the Lushan TTG-like gneisses. It had been suggested that rutile fractionation will cause high Nb/Ta ratios in the residual melts (Xiong et al., 2005; Klemme et al., 2006). However, more recent evidence from natural samples suggests that Nb/Ta ratio in rutile is quite variable (Aulbach et al., 2008). Rutiles from ancient and metasomatism subcontinental lithospheric mantle have superchondritic Nb/Ta ratios, but those from undisturbed residues would have subchondritic Nb/Ta ratios (Aulbach et al., 2008). The positive $\varepsilon_{Nd}(t)$ values and coupling Nd–Hf model ages without relic zircons in the Lushan TTG-like gneisses indicate the mostly undisturbed source. Removal of rutile with subchondritic Nb/Ta ratios may cause high Nb/Ta ratios in the residual melts, so the strong negative correlation between Nb/Ta and Ti/Ti* may indeed reflect the effect of rutile (Fig. 14f).

The Lushan TTG gneisses show depleted and concave-upward REE patterns between middle and heavy REEs, which are apparently the effect of amphibole removal by fractional crystallization or as a residual phase during melting because amphibole has high partition coefficients for these elements (Rollinson, 1993, and references therein). So amphibole as a liquidus phase during magma evolution or as a residual phase during melting can cause negative Ta–Nb and Ti anomalies in the Lushan TTG, which is also supported by distinct higher Zr/Sm in TTG gneisses than in TTG-like gneisses and primitive mantle (Fig. 14a). The Lushan TTG samples also have scattered Nb/Ta ratios, and high Nb/Ta ratios in some samples (TH05-9, TH05-16 and TH05-21; Fig. 14), which might be attributed to the buffering effect of plagioclase accumulation (Fig. 11). Thus the present data could not exclude the possibility of rutile as a residual phase during partial melting. Although amphibole fractionation is likely a very important process in the petrogenesis of the Lushan TTG, the predicted negative relationship between Zr/Sm and Ti/Ti* did not occur (Fig. 14e). Zircon fractionation may be the main reason when considering low Zr contents in the felsic samples (see Supplementary Table 3), which will also lower Y contents and raise Sr/Y ratios of the melts (Moyen, 2009).

5.3. Implications for the Archean crustal accretion at the Southern NCC

5.3.1. Ages of the Lushan amphibolite

The Lower Taihua group is the most important and extensive Archean terrane at the southern margin of the NCC (Zhang et al., 1985). The existing age data of the Taihua terrain include Sm–Nd isochron age of 2766 ± 29 Ma for whole-rock samples of the Lushan amphibolite (Xue et al., 1995) and U–Pb ages of 2806–2841 Ma for three zircon grains in a tonalitic gneiss sample (Kröner et al., 1988). Whole rock Sm–Nd isochron age of 2766 ± 29 Ma for the Lushan amphibolite (Xue et al., 1995) is the same as zircon SHRIMP U–Pb age of the Lushan TTG-like gneisses in this study. The geological observations show that amphibolites commonly occur as enclave in the Lushan gneisses, so the whole rock Sm–Nd isochron age of Xue et al. (1995) is likely to reflect the reset of the Sm–Nd isotope system related to magmatism of TTG-like rocks.

5.3.2. Original crustal accretion during 2.95–2.80 Ga

The Lushan amphibolites have low-SiO_2, high-MgO and Fe_2O_3 (Fig. 6) with variable $Mg^{\#}$ (0.41–0.65), relatively high TiO_2 and CaO, Cr (37.2–442 ppm), Ni (43.2–177 ppm) and V (197–369 ppm), which is consistent with the protoliths being basaltic rocks. Furthermore, the Lushan amphibolites have flat chondrite-normalized REE patterns, nearly flat primitive mantle-normalized trace-element spidergram without obvious Nb, Ta Ti and Eu anomalies, and positive $\varepsilon_{Nd}(t)$ of 1.20–3.25 (calculated to 2.77 Ga). These geochemical features further suggest that the protoliths may be E-MORB-like (Fig. 9b). If these amphibolites could be considered as representing the components of initial oceanic crust in the southern NCC, then the ocean crust would have formed at ~3.0 Ga (from 2.95 to 2.80 Ga) (Fig. 15a) according to the depleted mantle Nd model ages of amphibolites (2.8–3.0 Ga; Supplementary Table 4) and the oldest relict zircon (2.95 Ga) in the TTG gneisses.

The zircon SHRIMP U–Pb age of TH05-21 also suggests that the previous single grain zircon U–Pb ages (2806–2841 Ma; Kröner et al., 1988) would be mean ages of the mixture within single grain. These relic zircons might record the original crustal accretion in the area, perhaps during 2.95–2.80 Ga based on the $^{207}Pb/^{206}Pb$ ages and corresponding initial Hf isotopes of the relic zircons in TH05-21 (see Supplementary Table 1 and 2; Fig. 4). However, we do not yet know exactly the nature and origin of the early

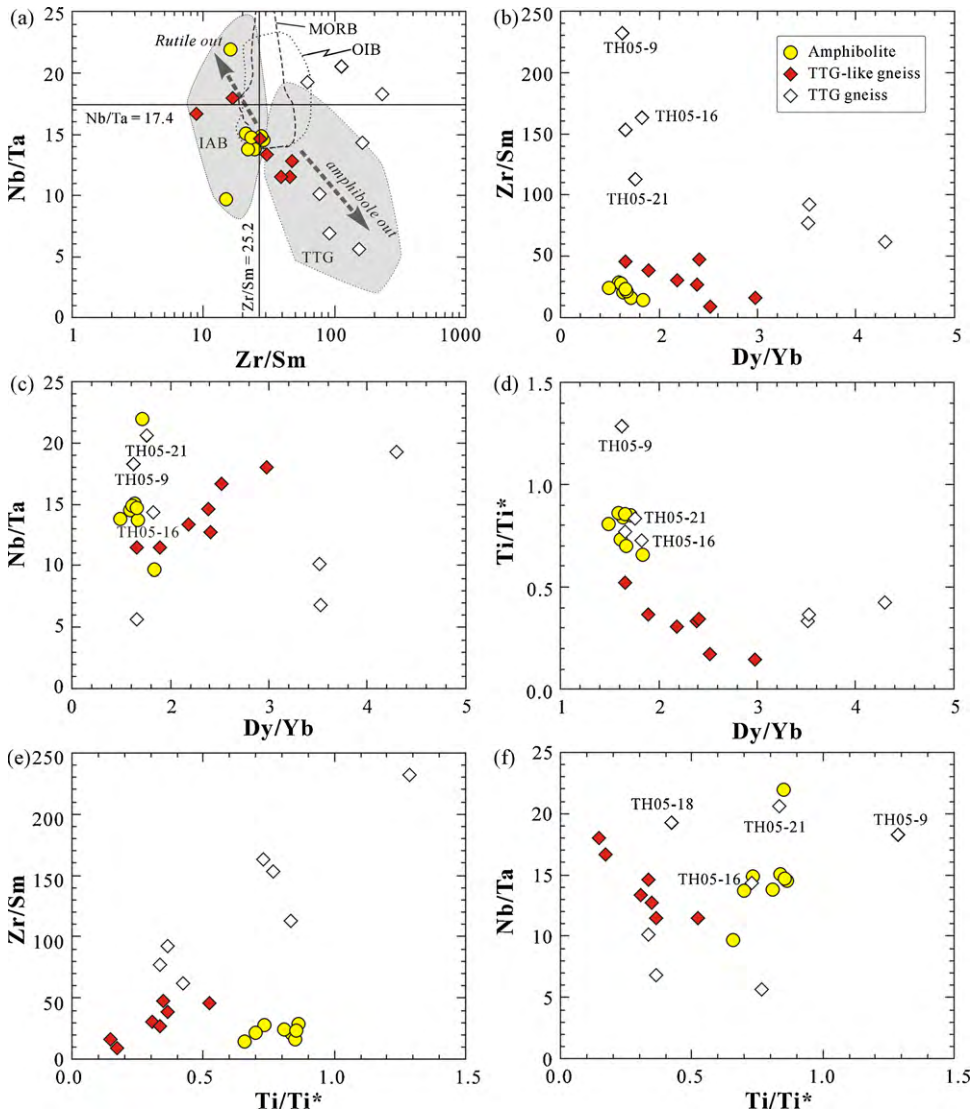

Fig. 14. (a) Nb/Ta vs. Zr/Sm, (b–d) Zr/Sm, Nb/Ta, Ti/Ti* vs. Dy/Yb and (e and f) Zr/Sm, Nb/Ta vs. Ti/Ti* diagrams for the Lushan gneisses and amphibolites. Fields of TTG, modern mid-ocean-ridge basalts (MORB), ocean-island basalts (OIB) and island arc basalt (IAB) are from Foley et al. (2002). Nb/Ta (17.4) and Zr/Sm (25.2) ratios of primitive mantle from Sun and McDonough (1989).

crustal materials in the southern NCC, whether sequential intra-oceanic thrust-stacking or obduction of oceanic crust (De Wit, 1998) (Fig. 15b) and/or accretion of oceanic plateaux (e.g., De Wit et al., 1992; Desrochers et al., 1993; Condie, 1997).

5.3.3. Flat-subduction at ~2.77 Ga

The subduction might be initially developed because of lateral compositional buoyancy contrast within the lithosphere (Niu et al., 2003). In the southern NCC, subsequent to the early preserved crust formed by intra-oceanic thrust-stacks and/or by accretion of oceanic plateau during 2.95–2.80 Ga, flat-subduction of oceanic slab because of high heat flow, as a significant mode of Archaean subduction (Abbott and Hoffman, 1984; Abbott, 1991; van Hunen et al., 2008), possibly began at ~2.77 Ga indicated by zircon SHRIMP U–Pb ages of the Lushan TGG-like gneisses. TTG melts produced through partial melting of subducted oceanic crust might have ascended and interacted with melts from peridotite in a thin mantle wedge, resulting in the low-SiO_2 and high-$Mg^{\#}$ TTG-like magmas that may have intruded the overlying oceanic plateau and/or intra-oceanic thrust-stacks (Fig. 15c). Our preferred model of subducting oceanic crust melting and melt interaction with the mantle wedge implies that TTG-like magmas would not be influenced by possible processes like early differentiations during intra-oceanic plate stacking and/or oceanic plateau accretion. Therefore, the Lushan TTG-like gneisses would have positive $\varepsilon_{Nd}(t)$ values and coupled Nd–Hf model ages without relic zircons.

5.3.4. Crustal thickening at 2.72 Ga

All the processes such as flat-subduction, intra-oceanic plate stacking and/or oceanic plateau accretion would result in crustal thickening. If crustal thickening is rapid, the appropriate conditions (e.g., eclogite facies) for partial melting can be achieved before the crust dehydrates, which would result in low-$Mg^{\#}$ and high SiO_2 TTG (Smithies and Champion, 2000). The Lushan TTG might result from melting of thickened lower crust (Fig. 15d-1) or together with underthrusting slabs locally excluding the mantle wedge (Fig. 15d-2). If the melt parental to the TTG were indeed derived from the thickened lower crust with complex differentiation histories during early intra-oceanic plate stacking and/or oceanic plateau accretion (Fig. 14b), the TTG would have complex relic zircons and negative $\varepsilon_{Nd}(t)$ values.

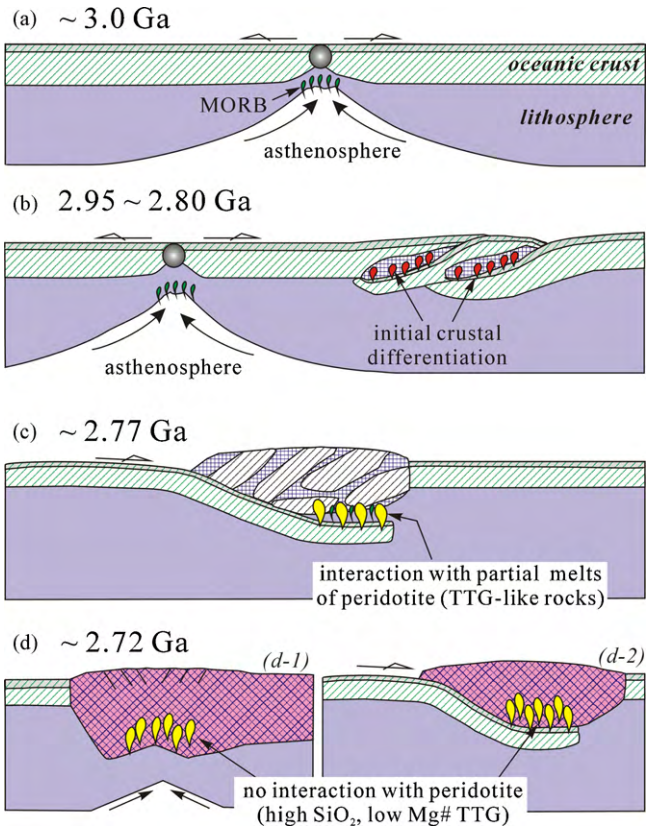

Fig. 15. Schematic diagram illustrating the tectonic scenario for the late Archean crustal evolution of the southern North China Craton.

5.4. Implications for the genesis of Archean TTGs

TTGs are the major component of the Archean crust (Smithies, 2000; Condie, 2005), which differ from the modern adakite by having lower $Mg^{\#}$, Cr, Ni and higher SiO_2 (Smithies, 2000; Martin et al., 2005; Condie, 2005). Because the composition of these TTGs is not consistent with modern-style subduction processes, melting of hydrous basaltic material at the base of thickened crust is perhaps more likely (Smithies, 2000). The observation that low-$Mg^{\#}$ and high SiO_2 TTG is dominant in the late Archean also supports the thickened lower crust model. However, geochemical features of Archean TTG magmas changed from 4.0 to 2.5 Ga (Martin et al., 2005; Condie, 2005), and late Archean TTGs were also thought to form principally above subduction zones (e.g., Drummond and Defant, 1990; Drummond et al., 1996; Martin, 1999; Rapp et al., 2003; Martin et al., 2005). Thus a critical issue related to TTGs is whether and how its genetic mechanism changes with time (Condie, 2005). The different origins of the Lushan TTG-like and TTG gneisses in the southern NCC record a transition from subduction to thickened crust.

There is wide acceptance that some form of plate tectonics was active in the Archean (e.g., Hoffman, 1989; Card, 1990; De Wit et al., 1992; Kröner and Layer, 1992; Hamilton, 1995). Therefore it seems reasonable to suggest that TTG may have formed in a subduction environment (e.g., Drummond and Defant, 1990; Drummond et al., 1996; Martin, 1999; Rapp et al., 2003; Martin et al., 2005). High-$Mg^{\#}$ and low-SiO_2 TTG-like gneiss in the Lushan Lower Taihua complex show the geochemical characteristics in favor of the subducting oceanic slab model, which highlights the possibility of subduction environment for TTG formation during the late Archean.

The generation of high-$Mg^{\#}$ and low-SiO_2 TTG requires slab melting at great depth and interaction of the melt with the mantle wedge (e.g., Martin, 1999; Smithies, 2000; Smithies and Champion, 2000; Martin et al., 2005; Condie, 2005). Therefore, production of high-$Mg^{\#}$ and low-SiO_2 TTG would be less likely if subduction was typically flat without mantle wedge. Additionally, the short time interval between the generation of the Lushan TTG-like rocks (2765 ± 13 Ma) and TTG (2723 ± 9 Ma) suggests that the condition of flat-subduction with a mantle wedge in the Archean might be short-lived, which may help explain the absence of high-$Mg^{\#}$ and low-SiO_2 TTG in most Archean terranes.

6. Conclusions

On the basis of geochronological, geochemical and Nd–Hf isotopic data, the following conclusions can be drawn on the petrogenesis of the Lushan Lower Taihua complex:

(1) The Lower Taihua complex at Lushan area is dominated by amphibolite, TTG-like gneisses (2765 ± 13 Ma) and TTG gneisses (2723 ± 9 Ma). The TTG gneisses contain abundant relic zircons with ages between 2.95 and 2.80 Ga.
(2) The high-$Mg^{\#}$ and low-SiO_2 TTG-like gneisses may have derived from partial melting of flat-subducting ocean crust and the melt interaction with the mantle wedge. The low-$Mg^{\#}$ and high SiO_2 TTG gneisses resulted from partial melting of thickened lower crust composed of older materials differentiated during early crustal accretion, which had undergone plagioclase accumulation and garnet ± amphibole fractionation.
(3) Geochronological, geochemical and Nd–Hf isotopic data of the gneisses from the Lushan Lower Taihua complex record the history of Archean crustal accretion in the southern NCC from ocean crust formation to subducting-slab melting, and to intracrustal reworking.

Acknowledgements

We gratefully acknowledge the careful and constructive comments of Professor W. Mueller and three anonymous reviewers, which considerably improved the manuscript. We appreciate Y. Liu, X.L. Tu, X.R. Liang, B. Song (Beijing SHRIMP Center) and H.H. Zhang for assistance in major element, trace element, Nd isotope analyses, zircon U–Pb dating and Lu–Hf isotope analyses, respectively. The research was supported by the National Natural Science Foundation of China (NSFC Projects 90714001, 40573015), Knowledge Innovation Project of the Chinese Academy of Sciences (KZCX2-YW-Q08-3-6) and the CAS/SAFEA International Partnership Program for Creative Research Teams. This is contribution no. IS-1212 from GIG-CAS.

Appendix A. Supplementary data

Supplementary data associated with this article can be found, in the online version, at doi:10.1016/j.precamres.2010.06.020.

References

Abbott, D., 1991. The case for accretion of the tectosphere by buoyant subduction. Geophys. Res. Lett. 18, 585–588.
Abbott, D.H., Hoffman, S.E., 1984. Archaean plate tectonics revisited. 1. Heat flow, spreading rate, and the age of subducting oceanic lithosphere and their effects on the origin and the evolution of continents. Tectonics 3, 429–448.
Aulbach, S., O'Reilly, S.Y., Griffin, W.L., Pearson, N.J., 2008. Subcontinental lithospheric mantle origin of high niobium/tantalum ratios in eclogites. Nat. Geosci. 1, 468–472.
Barker, F., 1979. Trondhjemite: definition, environment and hypotheses of origin. In: Barker, F. (Ed.), Trondhjemites Dacites and Related Rocks. Elsevier, Amsterdam, pp. 1–12.
Barker, F., Arth, J.G., 1976. Generation of trondhjemitic–tonalitic liquids and Archaean bimodal trondhjemite–basalt suites. Geology 4, 596–600.

Barth, M.G., Foley, S.F., Horn, I., 2002. Partial melting in Archean subduction zones: constraints from experimentally determined trace element partition coefficients between eclogitic minerals and tonalitic melts under upper mantle conditions. Precamb. Res. 113, 323–340.
Bédard, J.H., 2006. A catalytic delamination-driven model for coupled genesis of Archaean crust and sub-continental lithospheric mantle. Geochim. Cosmochim. Acta 70, 1188–1214.
BGMR (Bureau of Geology and Mineral Resources), 1965. Geological map of Henan Province. Sheet I-49-XXIII (Lushan), scale 1:200,000. Zhengzhou.
Card, K.D., 1990. Areview of the Superior Province of the Canadian Shield, a product of Archean accretion. Precamb. Res 48, 99–156.
Castillo, P.R., Janney, P.E., Solidum, R.U., 1999. Petrology and geochemistry of Camiguin island, southern Philippines: insights to the source of adakites and other lavas in a complex arc setting. Contrib. Mineral. Petrol. 134, 33–51.
Coltorti, M., Bonadiman, C., Faccini, B., Grégoire, M., O'Reilly, S.Y., Powell, W., 2007. Amphiboles from suprasubduction and intraplate lithospheric mantle. Lithos 99, 68–84.
Condie, K.C., 1997. Contrasting sources for upper and lower continental crust: the greenstone connection. J. Geol. 105, 729–736.
Condie, K.C., 2005. TTGs and adakites: are they both slab melts? Lithos 80, 33–44.
Davidson, J., Macpherson, C., Turner, S., 2007. Amphibole control in the differentiation of arc magmas. Geochim. Cosmochim. Acta 71, A204.
De Wit, M.J., 1998. On Archean granites, greenstones, cratons and tectonics: does the evidence demand a verdict? Precamb. Res. 91, 181–226.
De Wit, M.J., Roering, C., Hart, R.J., Armstrong, R.A., de Ronde, C.E.J., Green, R.W.E., Tredoux, M., Peberdy, E., Hart, R.A., 1992. Formation of an Archaean continent. Nature 357, 553–562.
Defant, M.J., Drummond, M.S., 1990. Derivation of some modern arc magmas by melting of young subducted lithosphere. Nature 347, 662–665.
Desrochers, J.P., Hubert, C., Ludden, J., Pilote, P., 1993. Accretion of Archean oceanic plateau fragments in the Abitibi greenstone belt, Canada. Geology 21, 451–454.
Drummond, M.S., Defant, M.J., 1990. A model for trondhjemite–tonalite–dacite genesis and crustal growth via slab melting: Archean to modern comparisons. J. Geophys. Res. 95, 21503–21521.
Drummond, M.S., Defant, M.J., Kepezhinskas, P.K., 1996. Petrogenesis of slab-derived trondhjemite–tonalite–dacite/adakite magmas. Transactions of the Royal Society of Edinburgh. Earth Sci. 87, 205–215.
Foley, S.F., Venturelli, G., Green, D.H., Toscani, L., 1987. The ultrapotassic rocks: characteristics, classification, and constraints for petrogenetic models. Earth Sci. Rev. 24, 81–134.
Foley, S., Tiepolo, M., Vannucci, R., 2002. Growth of early continental crust controlled by melting of amphibolite in subduction zones. Nature 417, 837–840.
Griffin, W.L., Pearson, N.J., Belousova, E.A., Saeed, A., 2006. Comment: Hf-isotope heterogeneity in zircon 91500. Chem. Geol. 233, 358–363.
Griffin, W.L., Pearson, N.J., Belousova, E., Jackson, S.E., O'Reilly, S.Y., van Achterberg, E., Shee, S.R., 2000. The Hf isotope composition of cratonic mantle: LAM-MC-ICPMS analysis of zircon megacrysts in kimberlites. Geochim. Cosmochim. Acta 64, 133–147.
Hamilton, W.B., 1995. Subduction systems and magmatism. In: Smellie, J.L. (Ed.), Volcanism Associated with Extension at Consuming Plate Margins. Geological Society, London, pp. 3–28, Special Publications 81.
Hofmann, A.W., 1988. Chemical differentiation of the earth: the relationship between mantle, continental crust, and oceanic crust. Earth Planet. Sci. Lett. 90, 297–314.
Hoffman, P.F., 1989. Precambrian geology and tectonic history of North America. In: Bally, A.W., Palmer, A.R. (Eds.), The Geology of North America: An Overview. Geological Society of America, Boulder, pp. 447–512.
Huang, X., Bai, Z., DePaolo, D.J., 1986. Sm–Nd isotope study of early Archean rocks, Qianan, Hebei Province, China. Geochim. Cosmochim. Acta 50, 625–631.
Huang, X.L., Xu, Y.G., Liu, D.Y., 2004. Geochronology, petrology and geochemistry of the granulite xenoliths from Nushan, east China: implication for a heterogeneous lower crust beneath the Sino-Korean craton. Geochim. Cosmochim. Acta 68, 127–149.
Huang, X.L., Xu, Y.G., Lan, J.B., Yang, Q.J., Luo, Z.Y., 2009. Neoproterozoic adakitic rocks from Mopanshan in the western Yangtze Craton: partial melts of a thickened lower crust. Lithos 112, 367–381.
Ionov, D.A., Hofmann, A.W., 1995. Nb–Ta-rich mantle amphiboles and micas: implications for subduction-related metasomatic trace element fractionations. Earth Planet. Sci. Lett. 131, 341–356.
Jahn, B.M., Auvray, B., Cornichet, J., Bai, Y.D., Shen, Q.H., Liu, D.Y., 1987. 3.5 Ga old amphibolites from eastern Hebei Province, China: field occurrence, petrography, Sm–Nd isochron age and REE geochemistry. Precamb. Res. 34, 311–346.
Jahn, B.M., Auvray, B., Shen, Q.H., Liu, D.Y., Zhang, Z.Q., Dong, Y.J., Ye, X.J., Zhang, Q.Z., Cornichet, J., Mace, J., 1988. Archean crustal evolution in China: the Taishan Complex and evidence for Juvenile crustal addition from long-term depleted mantle. Precamb. Res. 38, 381–403.
Jahn, B.M., Glikson, A.Y., Peucat, J.-J., Hickman, A.H., 1981. REE geochemistry and isotopic data of Archaean silicic volcanics and granitoids from the Pilbara Block, western Australia: implications for the early crustal evolution. Geochim. Cosmochim. Acta 45, 1633–1652.
Jahn, B.M., Zhang, Z.Q., 1984. Archean granulite gneisses from eastern Hebei Province, China: rare earth geochemistry and tectonic implications. Contrib. Mineral. Petrol. 85, 224–243.
Kay, S.M., Ramos, V.A., Marquez, M., 1993. Evidence in Cerro Pampa volcanic rocks for slab-melting prior to ridge-trench collision in southern South America. J. Geol. 101, 703–714.
Klemme, S., Gunther, D., Hametner, K., Prowatke, S., Zack, T., 2006. The partitioning of trace elements between ilmenite, ulvospinel, armalcolite and silicate melts with implications for the early differentiation of the moon. Chem. Geol. 234, 251–263.
Klemme, S., Prowatke, S., Hametner, K., Gunther, D., 2005. Partitioning of trace elements between rutile and silicate melts: implications for subduction zones. Geochim. Cosmochim. Acta 69, 2361–2371.
Kröner, A., Layer, P.W., 1992. Crust formation and plate motion in the early Archean. Science 256, 1405–1411.
Kröner, A., Compston, W., Zhang, G.W., Guo, A.L., Todt, W., 1988. Ages and tectonic setting of Late Archean greenstone–gneiss terrain in Henan Province, China, as revealed by single-grain zircon dating. Geology 16, 211–215.
Li, X.H., 1997. Geochemistry of the Longsheng Ophiolite from the southern margin of Yangtze Craton, SE China. Geochem. J. 31, 323–337.
Li, X.H., Li, Z.X., Ge, W.C., Zhou, H.W., Li, W.X., Liu, Y., Wingate, M.T.D., 2004. Reply to the comment: mantle plume, but not arc-related Neoproterozoic magmatism in South China. Precamb. Res. 132, 405–407.
Li, X.H., Li, Z.X., Wingate, M.T.D., Chung, S.L., Liu, Y., Lin, G.C., Li, W.X., 2006. Geochemistry of the 755 Ma Mundine Well dyke swarm, northwestern Australia: part of a Neoproterozoic mantle superplume beneath Rodinia? Precamb. Res. 146, 1–15.
Li, X.H., Li, Z.X., Zhou, H.W., Liu, Y., Kinny, P.D., 2002. U–Pb zircon geochronology, geochemistry and Nd isotopic study of Neoproterozoic bimodal volcanic rocks in the Kangdian Rift of South China: implications for the initial rifting of Rodinia. Precamb. Res. 113, 135–154.
Macpherson, C.G., Dreher, S., Thirlwall, M.F., 2006. Adakites without slab melting: high pressure differentiation of island arc magma, Mindanao, the Philippines. Earth Planet. Sci. Lett. 243, 581–593.
Martin, H., 1994. The Archean grey gneisses and the genesis of the continental crust. In: Condie, K.C. (Ed.), The Archean Crustal Evolution, Developments in Precambrian Geology. Elsevier, Amsterdam, pp. 205–259.
Martin, H., 1999. Adakitic magmas: modern analogues of Archaean granitoids. Lithos 46, 411–429.
Martin, H., Smithies, R.H., Rapp, R., Moyen, J.F., Champion, D., 2005. An overview of adakite, tonalite–trondhjemite–granodiorite (TTG), and sanukitoid: relationships and some implications for crustal evolution. Lithos 79, 1–24.
McKay, G., Le, L., Wagstaff, J., Crozaz, G., 1994. Experimental partitioning of rare earth elements and strontium: constraints on petrogenesis and redox conditions during crystallization of Antarctic angrite Lewis Cliff 86010. Geochim. Cosmochim. Acta 58, 2911–2919.
Moyen, J.-F., 2009. High Sr/Y and La/Yb ratios: the meaning of the "adakitic signature". Lithos 112, 556–574.
Niu, Y.L., O'Hara, M.J., 2009. MORB mantle hosts the missing Eu (Sr, Nb, Ta and Ti) in the continental crust: new perspectives on crustal growth, crust-mantle differentiation and chemical structure of oceanic upper mantle. Lithos 112, 1–17.
Niu, Y.L., O'Hara, M.J., Pearce, J.A., 2003. Initiation of subduction zones as a consequence of lateral compositional buoyancy contrast within the lithosphere: a petrological perspective. J. Petrol. 44, 851–866.
Rapp, P.R., Watson, E.B., Miller, C.F., 1991. Partial melting of amphibolite/eclogite and the origin of Archean trondhjemites and tonalites. Precamb. Res. 51, 1–25.
Rapp, R.P., Shimizu, N., Norman, M.D., 2003. Growth of early continental crust by partial melting of eclogite. Nature 425, 605–609.
Rollinson, H.R., 1993. Using Geochemical Data: Evaluation, Presentation, Interpretation. Longman Singapore Publishers (Pte) Ltd., Singapore, pp. 352.
Rudnick, R.L., Gao, S., 2003. The composition of the continental crust. In: Rudnick, R.L. (Ed.), The Crust. Treatise on Geochemistry, vol. 3. Elsevier, Oxford, pp. 1–64.
Shaw, D.M., 1968. A review of K–Rb fractionation trends by co-variance analysis. Geochim. Cosmochim. Acta 32, 573–602.
Shirey, S.B., Hanson, G.N., 1984. Mantle derived Archaean monzodiorites and trachyandesites. Nature 310, 222–224.
Sisson, T.W., 1994. Gornblende-melt trace-element partitioning measured by ion microprobe. Chem. Geol. 117, 331–344.
Smithies, R.H., Champion, D.C., 2000. The Archaean high-Mg diorite suite: links to tonalite-trondhjemite-granodiorite magmatism and implications for early Archaean crustal growth. J. Petrol. 41, 1653–1671.
Smithies, R.H., Champion, D.C., Van Kranendonk, M.J., 2009. Formation of Paleoarchean continental crust through infracrustal melting of enriched basalt. Earth Planet. Sci. Lett. 281, 298–306.
Smithies, R.H., 2000. The Archaean tonalite–trondhjemite–granodiorite (TTG) series is not an analogue of Cenozoic adakite. Earth Planet. Sci. Lett. 182, 115–125.
Steenfelt, A., Garde, A.A., Moyen, J.-F., 2005. Mantle wedge involvement in the petrogenesis of Archaean grey gneisses in West Greenland. Lithos 79, 207–228.
Sun, D.Z., Hu, H.F., 1993. The Tectonic Framework of Precambrian in Zhongtiaoshan. Geol. Publ. House, Beijing, pp. 250 (in Chinese with English abstract).
Sun, M., Armstrong, R.L., Lambert, R.S.J., 1992. Petrochemistry and Sr, Pb and Nd isotopic geochemistry of Early Precambrian rocks, Wutaishan and Taihangshan areas, China. Precamb. Res. 56, 1–31.
Sun, S.-S., McDonough, W.F., 1989. Chemical and isotopic systematics of oceanic basalts: implications for mantle composition and processes. In: Saunders, A.D., Norry, M.J. (Eds.), Magmatism in the Ocean Basins. Geol. Soc. Spec. Publ. 42, pp. 313–345.
Tanaka, T., Togashi, S., Kamioka, H., Amakawa, H., Kagami, H., Hamamoto, T., Yuhara, M., Orihashi, Y., Yoneda, S., Shimizu, H., Kunimaru, T., Takahashi, K., Yanagi, T., Nakano, T., Fujimaki, H., Shinjo, R., Asahara, Y., Tanimizu, M., Dragusanu, C., 2000. JNdi-1: a neodymium isotopic reference in consistency with LaJolla neodymium. Chem. Geol. 168, 279–281.

Taylor, S.R., McLennan, S.M., 1985. The Continental Crust: Its Composition and Evolution. Blackwell, Oxford.
Tiepolo, M., Bottazzi, P., Foley, S.F., Oberti, R., Vannucci, R., Zanetti, A., 2001. Fractionation of Nb and Ta from Zr and Hf at mantle depths: the role of titanian pargasite and kaersutite. J. Petrol. 42, 221–232.
Tiepolo, M., Vannucci, R., Oberti, R., Foley, S., Bottazzi, P., Zanetti, A., 2000. Nb and Ta incorporation and fractionation in titanian pargasite and kaersutite: crystal chemical constraints and implications for natural systems. Earth Planet. Sci. Lett. 176, 185–201.
Tu, S.X., 1998. Geochemical comparing of two types of amphibolites within Taihua Group in Lushan County, Henan Province and their tectonic setting. Geochimica 27, 412–421 (in Chinese with English abstract).
van Hunen, J., van Keken, P.E., Hynes, A., Davies, G.F., 2008. Tectonics of early earth: some geodynamic considerations. Geol. Soc. Am. Spec. Paper 440, 157–171.
Wan, Y.S., Wilde, S.A., Liu, D.Y., Yang, C.X., Song, B., Yin, X.Y., 2006. Further evidence for ~1.85 Ga metamorphism in the Central Zone of the North China Craton: SHRIMP U–Pb dating of zircon from metamorphic rocks in the Lushan area, Henan Province. Gondwana Res. 9, 189–197.
Wang, Q., Xu, J.F., Jian, P., Bao, Z.W., Zhao, Z.H., Li, C.F., Xiong, X.L., Ma, J.L., 2006. Petrogenesis of adakitic porphyries in an extensional tectonic setting, Dexing, South China: implications for the genesis of porphyry copper mineralization. J. Petrol. 47, 119–144.
Williams, I.S., 1998. U–Th–Pb geochronology by ion microprobe. In applications of microanalytical techniques to understanding mineralizing processes. Rev. Econ. Geol. 7, 1–35.
Wu, F.Y., Yang, Y.H., Xie, L.W., Yang, J.H., Xu, P., 2006. Hf isotopic compositions of the standard zircons and baddeleyites used in U–Pb geochronology. Chem. Geol. 234, 105–126.
Wu, F.Y., Zhang, Y.B., Yang, J.H., Xie, L.W., Yang, Y.H., 2008. Zircon U–Pb and Hf isotopic constraints on the Early Archean crustal evolution in Anshan of the North China Craton. Precamb. Res. 167, 339–362.
Wu, J.S., Geng, Y.S., Shen, Q.H., Wan, Y.S., Liu, D.Y., Song, B., 1998. Archaean Geology Characteristics and Tectonic Evolution of China–Korea Paleo-continent. Geol. Publ. House, Beijing, pp. 211 (in Chinese).
Xiong, X.L., Adam, J., Green, T.H., 2005. Rutile stability and rutile/melt HFSE partitioning during partial melting of hydrous basalt: implications for TTG genesis. Chem. Geol. 218, 339–359.
Xu, P., Wu, F., Xie, L., Yang, Y., 2004. Hf isotopic compositions of the standard zircons for U–Pb dating. Chin. Sci. Bull. 49, 1642–1648.
Xue, L.W., Yuan, Z.L., Zhang, Y.S., Qiang, L.Z., 1995. The Sm–Nd isotope age of Taihua Group in Lushan area and their implications. Geochimica 24, Suppl., 92–97 (in Chinese with English abstract).
Yang, J.H., Wu, F.Y., Wilde, S.A., Zhao, G.C., 2008. Petrogenesis and geodynamics of Late Archean magmatism in eastern Hebei, eastern North China Craton: geochronological, geochemical and Nd–Hf isotopic evidence. Precamb. Res. 167, 125–149.
Zhang, G.W., Bai, Y.B., Song, Y., Guo, A.L., Zhou, D.W., Li, T.H., 1985. Composition and evolution of the Archean crust in central Henan, China. Precamb. Res. 27, 7–35.
Zhao, G.C., Cawood, P.A., Wilde, S.A., Lu, L.Z., 2000. Metamorphism of basement rocks in the Central Zone of the North China Craton: implications for Paleoproterozoic tectonic evolution. Precamb. Res. 103, 55–88.
Zhao, G.C., Sun, M., Wilde, S.A., Li, S.Z., 2005. Late Archean to Paleoproterozoic evolution of the North China Craton: key issues revisited. Precamb. Res. 136, 177–202.
Zhao, G.C., Wilde, S.A., Cawood, P.A., Sun, M., 2001. Archean blocks and their boundaries in the North China Craton: lithological geochemical, structural and P–T path constraints and tectonic evolution. Precamb. Res. 107, 45–73.
Zhao, G.C., Wilde, S.A., Cawood, P.A., Sun, M., 2002. SHRIMP U–Pb zircon ages of the Fuping complex: implications for Late Archean to Paleoproterozoic accretion and assembly of the North China Craton. Am. J. Sci. 302, 191–226.